2011 International Nuclear Atlantic Conference - INAC 2011
Belo Horizonte,MG, Brazil, October 24-28, 2011
ASSOCIAÇÃO BRASILEIRA DE ENERGIA NUCLEAR - ABEN
ISBN: **978-85-99141-04-5**

Chitosan Microspheres loaded with holmium-165 produced by Spray Dryer for liver cancer therapy: preliminary experiments

Douglas Massao Miyamoto*[1], Geovanna Pires[1], Raphael A. de Lira[1], Vitor H.S. Melo[1], João Alberto Osso Junior[2], Nanci Nascimento[1], Mariangela de Burgos M. de Azevedo[1].
Instituto de Pesquisas Energéticas e Nucleares (IPEN), Brazil.

[1] Instituto de Pesquisas Energéticas e Nucleares (IPEN / CNEN - SP)
Av. Professor Lineu Prestes 2242
05508-000 São Paulo, SP
*e-*mail:* douglas.miyamoto@usp.br

[2] Centro de Radiofarmácia (IPEN / CNEN - SP)
Av. Professor Lineu Prestes 2242
05508-000 São Paulo, SP

ABSTRACT

Chitosan is a biopolymer of 2-deoxy-2-amino-D-glucose that is obtained by deacetylation of chitin. It's biocompatible, biodegradable, non toxic and has antitumor activity. Chitosan has many applications, such as their microparticles that can be used to treat prostate cancer, rheumatoid arthritis, and for liver tumor brachytherapy treatment [1,2,3,4,5]. Our group is developing different biodegradable polymer-based microspheres loaded with holmium-165 for this purpose [6].
The Chitosan microspheres were produced loaded with holmium (III) chloride, and not loaded with it, by Mini Spray Dryer procedure.
The microspheres were evaluated by scanning electron microscopy (SEM), Energy Dispersive Spectroscopy (EDS), Confocal laser scanning microscopy (CLSM), Thermogravimetric analysis (TGA), Particle Size, and X-ray Diffraction (XRD). The EDS analysis confirmed the holmium chloride presence into the prepared chitosan microparticles.

1. INTRODUCTION

Chitosan has many interesting biological properties as biodegradability, biocompatibility, absorptive, non-toxicity and polyelectrolyte characteristics [7]. It is a carbohydrate linear copolymer chain with a higher percentage of 2-amino-2-deoxy-D-glucopyranoside relative to 2-acetamido-2-deoxy-D-glucopyranoside, which are joined by β(1-4) glycosidic bonds. It is soluble in acidic aqueous media, but is insoluble in neutral and alkaline ones [8]. By the other side, the poly(vinyl alcohol) or (PVA) is a water soluble polymer, biocompatible and biodegradable too, and industrially obtained by alkaline hydrolysis of poly(vinyl acetate). It can be acquired in several degrees of hydrolysis and polymerization [9]. The chitosan and PVA microgels or microspheres exhibits favorable drug controlled release properties, better comfort, reduced irritation in tissues, facilitated processing conditions, improved flexibility and an enhanced dissolution [10]. Glutaraldehyde has been commonly used in many cross-linking procedures, forming Schiff bases reacting with amino groups of chitosan (figure 1a) or acetal bridges in PVA (figure1b) [11].

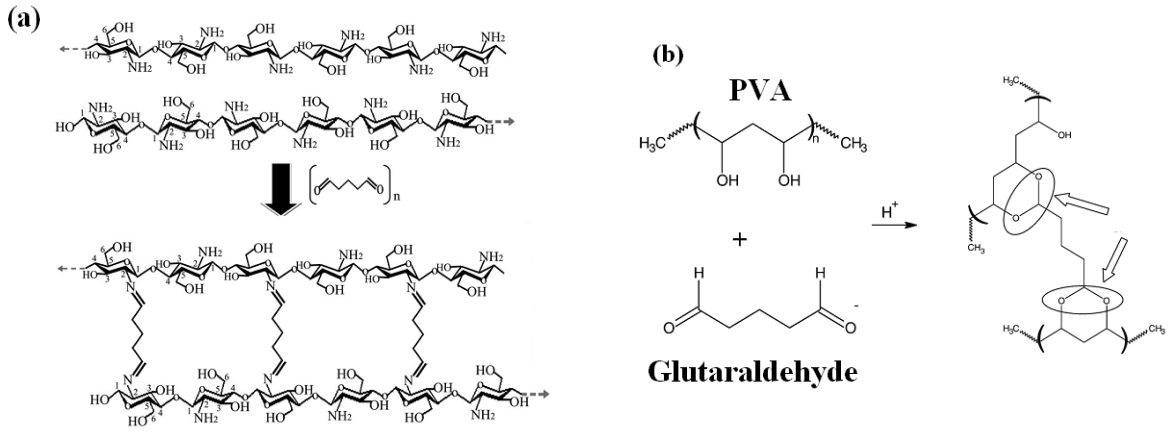

Figure 1: (a) reaction between chitosan and glutaraldehyde [14] (Copyright); (b) reaction between PVA and glutaraldehyde [12] (Copyright).

Increased structural and chemical stability of such cross-linked derivatives contributes to their resistance and acid endurance from surface. Cross-linking chitosan with glutaraldehyde creates a three-dimensional network within the biopolymer, and increases the internal surface area for metal adsorption [11].

There are many macromolecular structures that are possible for hydrogels, like cross-linked or entangled as *Interpenetrating Polymer Networks* (IPNs), *Hybrid Polymer Networks* (HPNs), linear homopolymers, linear copolymers and the block copolymers (or graphitized). They can also be made of polymeric ion valence multiple, complex hydrogen bond networks or stabilized by hydrophilic domains, hydrophobic stabilized ones, and physical blends. IPNs are unique types of polymer alloys consisting of two or more cross-linked polymers with no covalent bonds (grafts) between them [13,14]. Once these intimate mixtures are held together by permanent entanglements they are polymeric catenates, produced by homocross-linking of two or more polymer systems which can be prepared by "sequential" or "simultaneous" technique. When linear polymers are combined with cross-linked ones, in various degrees of interpenetration, it is formed a pseudo or semi-IPN [15,16]. Finally, several interactions possibilities can occur between the polymer networks that form a HPN and the most common one is the occurrence of covalent interactions between networks through a inter-cross-linking, in with cross-linking agents form covalent bonds with the different polymers [8,17].

Spray drying technology is widely known, used to transform rapidly and efficiently liquids (solutions, emulsions, suspension, slurries, pastes or even melts) in solid powders. Its main applications are found in the food, chemical and materials industries to enhance ingredient conservation, particle properties, powder handling and storage, etc. This technique can also be used for specific applications in the formulation of pharmaceuticals for drug delivery. With the development of active compounds and emulsion encapsulation actually used in pharmaceutics, cosmetics and functional food preparation, this method has also been used for encapsulation purposes. Powder thus generated is a matrix system (microparticles) exhibiting spherical or hollowed morphology depending on the nature of the wall material used and the operational drying conditions do evaluate such as: the inlet temperature, solid concentration, and gas flow rate or feed rate. The powder samples obtained are generally heterogeneous and amorphous [18].

2. EXPERIMENTAL

2.1. Materials

All chemicals were commercially available and used as obtained. Chitosan of high molecular weight, holmium (III) chloride hexahydrate and PVA 98-99% hydrolyzed were obtained from Sigma Aldrich. Glutaraldehyde 25% in water solution and acetic acid were obtained from VETEC.

2.2. Methods

2.2.1 Preparation of the Chitosan microspheres

Spray-drying can be used as one-step preparation of nanoparticle powders. Grenha et al [19] prepared mannitol microspheres containing protein loaded chitosan nanoparticles by this method. Huang et al [20] also using this method prepared chitosan-iron oxide nanoparticles with many biopolymer : metal oxide ratios; their atomic absorption spectrometry results implied that iron has strongly chelated by chitosan. The commercial glutaraldehyde solution was diluted 1:10 (v/v) in water to use, and chitosan microspheres were prepared according to the description shown in Table 1.

Table 1: The samples compositions and respectively methods are described. The parameters of Mini Spray Dryer Büchi B-290 used were bomb 40%, in let temperature 180ºC [21], out let temperature 90ºC. GLU- glutaraldehyde, the cross-link agent

Sample	*Chitosan*	*Acetic acid (v/v)*	*Holmium chloride*	*PVA solution 0.5% (w/v)*	*GLU*	*Shaking Time*
A	3g/300 mL	5%	--	--	--	12h
B	3g/300 mL	5%	0,5g	--	--	12h
C	3g/250 mL	5%	--	50 mL	--	12 h
D	3g/250 mL	5%	0,5g	50 mL	--	12 h
E	3g/250 mL	5%	--	50 mL	3 mL	12h + 1h GLU
F	3g/250 mL	5%	0,5g	50 mL	3 mL	12h + 1h GLU

2.3. Characterization

Thermogravimetric measurement (TG) was recorded with a Mettler-Toledo TGA/SDTA 851 thermobalance in nitrogen atmosphere, from 25 up to 600 °C, and heating rate of 10 °C min^{-1}.

The SEM images were obtained in a Phillips XL 30 Microscope and equipment JEOL model JSM-7401 with an operating voltage of 1.0 kV in magnitude of 2,500 X using samples not covered and covered with carbon in a Sputter Coater BAL-TEC SCD 050.

Fourier Transform Infrared Spectroscopy (FTIR) was performed at Nicolet 6700 FT-IR spectrometer equipped with ATR and at BOMEM MB-100 Economical High Performance FTIR (pellets with KBr were used in the proportion 100:4 KBr/sample (w/w); samples were

dried at 100° C for 48h before pellets preparation). Spectra were measured in transmittance mode, in a wavenumber range of 4000-400 cm^{-1}.

Confocal Laser Scanning Microscopy (CLSM) was obtained in a LSM 500 – Carl Zeiss. The excitation wavelength was 488 nm, and wavelength fluorescence observed is 505-530 nm.

X-Ray Diffraction (XRD) analyses were performed using a Rigaku diffractometer model Miniflex II using Cu Kα radiation source (l = 0.15406 nm). Diffractograms were recorded from 2θ = 05° to 50°, with a step size of 0.05° and scan time of 2s per step. The chitosan crystallinity index (ICR) in absence or presence of holmium can be determined by equation 1: IC and IA are the intensities of signals related to, respectively, crystalline and amorphous regions [22,23,24].

ICR = [(IC-IA)/IC].100% Equation 1 [22]

The chitosan microparticles sizes and distribution were measured by light scattering analysis using CILAS laser particle size analyzer equipment, with low flux, and ethanol was used as a dispersed medium.

The EDS Analysis was performed to confirm the presence of Holmium in samples (B), (D) and (F). Experimental conditions: for sample (B) it was used accelerating voltage of 20.0 kV, magnification of 10000x. In sample (D) it was used also a accelerating voltage of 20.0 kV, but a magnification of 2700x. Sample (F) required a filter Fit Chi Squared=1.358, Correction Method Proza (Phi-Rho-Z), acceleration voltage of 15.0 kV, angle of 29.8 deg and Pionner detector coupled to Phillips XL 30 Microscope and equipment JEOL model JSM-7401 .

3. RESULTS AND DISCUSSION

3.1. Morphology analysis by scanning electron microscopy (SEM)

Morphologically there isn't too much difference between pairs samples (A) and (B), or between (C) and (D) ones, as can be seen in figure 2(I), (II), (III), (IV). However, the samples (C) and (D) microspheres are much smoother than samples (A) and (B) ones. This is because when chitosan is dried the water that was interacting with the biopolymer by hydrogen bonds leaves empty spaces in the microsphere, explaining why the microspheres in samples (A) and (B) have porous surfaces resembling "brains". Samples (C) and (D) microspheres instead didn't show such morphology: very smoother and spherical particles compared to samples (A) and (B) ones are ascribed to the effects of PVA interacting with the chitosan. Once these polymers are very compatible, samples (C) and (D) microspheres didn't show any phase separation, a tendency confirmed also by DRX and TGA analysis done in items, respectively, 3.6 and 3.7.
The sample (F) showed in figure 2(VI) is also spherical, but the microparticles surface apparently rough is ascribed probably because is the only one covered with carbon. The sample (E), in figure 2(V), is not covered with carbon and its surface is smoother than (F). These microspheres have a macromolecular structure very different from the other ones prepared: chitosan and PVA were cross-linked by glutaraldehyde forming an HPN matrix, in which holmium salts are dispersed.

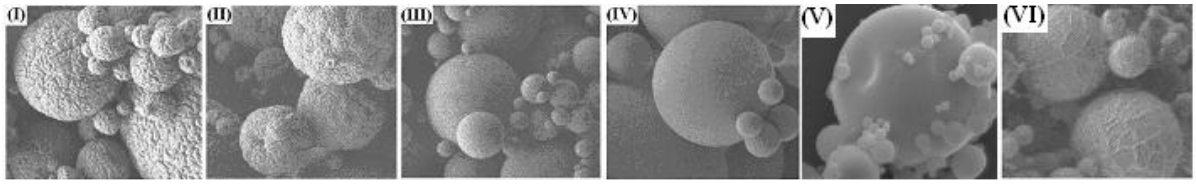

Figure 2: Scanning electron microscopy (SEM): (I) sample A, (II) sample B, (III) sample C; (IV) sample D, (V) sample E ; (VI) sample F – the only covered with carbon. Samples chemical composition are described in table 1.

3.2. Particle Size Measurements

The medium size of the chitosan microparticles measured by light scattering analysis reveals a range between 4.36-10.28 μm (Table 2), with an almost monodisperse distribution to each sample (figures 3(I) until 3(VI)).

Table 2. Medium size of chitosan microspheres related to the samples (A), (B), (C), (D), (E), (F).

Sample	*Average Particle Size (μm)*
(A)	**4.36**
(B)	**5.06**
(C)	**8.03**
(D)	**7.32**
(E)	**7.44**
(F)	**10.28**

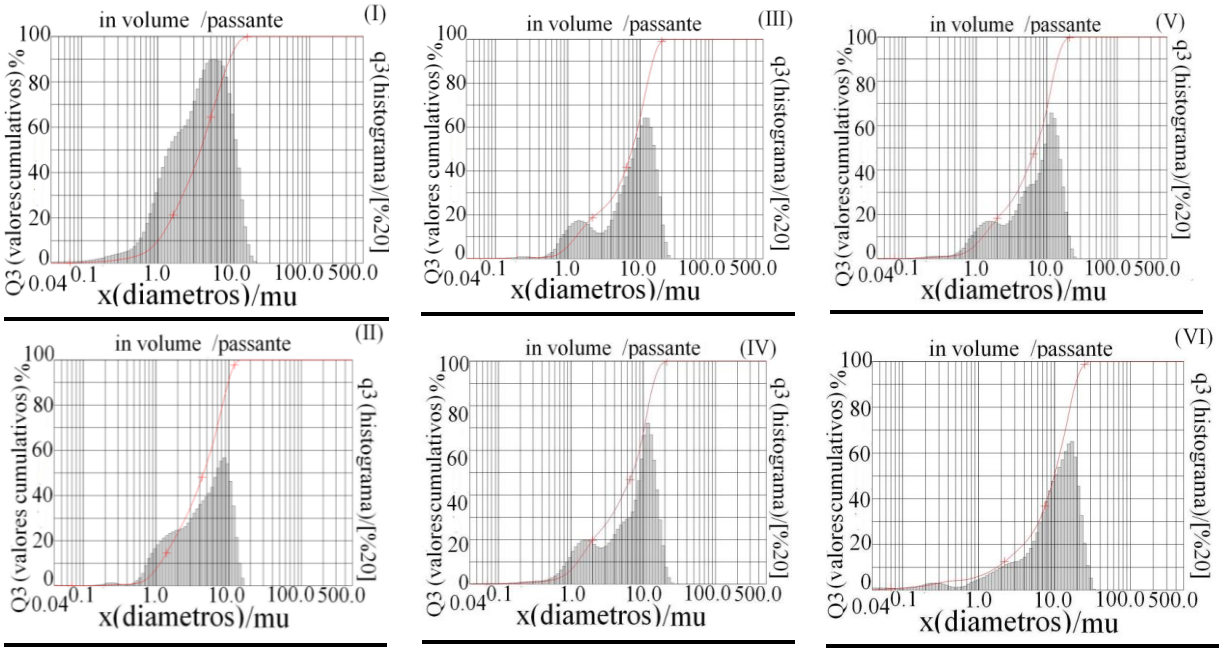

Figure 3. Particle size graphics of the samples: (I) A, (II) B, (III) C, (IV) D, (V) E, (VI) F, (samples are described in table 1).

It is underlined that comparing the pairs samples (A) and (B) - in this order, unload and $HoCl_3$ loaded chitosan microspheres, and (E) and (F) ones - respectively, unload and $HoCl_3$ loaded chitosan-PVA cross-linked microspheres - their average size become slightly larger increasing $HoCl_3$ content. In pair samples (A,B) the size gain was of 16,1 %, and to the pair (E,F) one it was of 38,2 %. Differences between such pair samples and (C, D) one probably is due PVA addition without a cross-link agent: there is no HPN, but a blend. Hydroxyl groups of PVA chains form hydrogen bonds with hydroxyl and amine groups of chitosan ones, replacing part of the bonds done by water molecules to define a structure stable but with water retained in places in which polymer chains are not so close. Hydroxyl and amine groups of chitosan, and hydroxyl ones in PVA, are chelating sites: as closer they are in free bending polymer chains as better the chelating site. It is well known that lanthanide ions have coordination spheres of 8-10 ligants due using "f" orbitals [25], so Ho^{+3} ions penetrating chain spaces inside the blend are likely to reach places to a strong chelation by even the both polymers. The inclusion of the lanthanide cation in the system of numerous chelate ligands occupying several coordination sites can change the dimension and/or type of the compound structure, in this case sample (D) is much more amorphous than sample(C) as showed in XRD of figure 9(I), the space inter polymer chains increase because of the hydrated metal ion salt dispersed in the matrix. But the hydroxyl groups in PVA aren't so good chelants as amine groups of chitosan, so it should indicate a tendency to form smaller particles in sample (D) than in sample (C), and explain why this is the only pair studied that showed smaller particles when have $HoCl_3$ dispersed in the matrix. The HPN cross-linked sample (F) has hydroxyl and amine groups which coordinate Ho^{+3} ions that are also involved in cross-link of chitosan and PVA, the amount of polymers to form microspheres must increase to compensate the loss of cross-link sites due chelating of the lanthanide to use all glutaraldehyde added. Additionally, cross-linked polymer networks have rigidily: in some places the bend is prohibitive due steric effects, hence a HPN may not be so packed as blends. Finally, Ho^{+3} coordination sphere can retain water molecules as its ligants, increasing microsphere volume. Comparing samples (E) and (F) one, after the PVA addition the hydrogel is stirred for 12h, and the only difference is the presence of holmium salt in sample (F) composition: after $HoCl_3$ was added, it was stirred for 12h, and the glutaraldehyde addiction was made after this and the final solution stirred for 1h as done in sample (E) preparation. The crosslink reaction occurred in a hydrogel with more space between the polymer chains, so the glutaraldehyde had more access to amine and hydroxyl groups, so the structure formed, including hydrated holmium salt, should be more rigid than in sample (E), what can explain the differences in particle size distribution.

The XDR analysis, item 3.6, offers more informations about this topic. The XRD patterns, figure 7(I), shows a strongest reflection at $2\theta = 20^o$ corresponds to polymorphic crystal *form II* (crystal structure also orthorhombic and its lattice parameters a = 4.4 Å, b= 10.0 Å, c= 10.3 (along fiber axis)[33] for all the samples without holmium in its composition. The figure 7(II) shows a reflection at $2\theta = 20^o$ smaller than in figure 7(I) and a weak reflection at $2\theta = 10^o$ in samples (B) and (D), but relatively strong in sample (F): according to Webster et al, the more the metal ion interact with amine groups, the more the peak around $2\theta = 10^o$ is intense; if this is related to existence of another crystallite when $HoCl_3$ is present in the matrix, this should explain the microparticles size distribution. The more intense is the peak around $2\theta = 10^o$, less dispersed is the microsphere size distribution. Consequently **HPN** $HoCl_3$ loaded cross-linked chitosan-PVA microsphere (sample (F)) is 38,2 % larger than a unloaded one (sample (E)); 40,4 % bigger related to a chitosan-PVA **blend** $HoCl_3$ loaded (sample (D)), and 28,1 % than a $HoCl_3$ unloaded one (sample (C)); and more than two times if compared to direct $HoCl_3$ unload and loaded chitosan microspheres like, respectively, samples (A) and (B).

3.3. Energy Dispersive Spectroscopy (EDS, or Energy Dispersive X-ray Spectroscopy)

The EDS Analysis can be done together with SEM, offering the first evidence of $HoCl_3$ load in the microspheres. Detection of chemical elements by x-rays depends of size and number of electrons of each atom, so Ho^{+3} and Cl^- ions have stronger signals related to the polymers used. The peaks of holmium III and chloride (hence, their load) in the samples (B), (D), (F) (whose composition in table 1), as can be observed in the figures 4(I), (II) and (III).

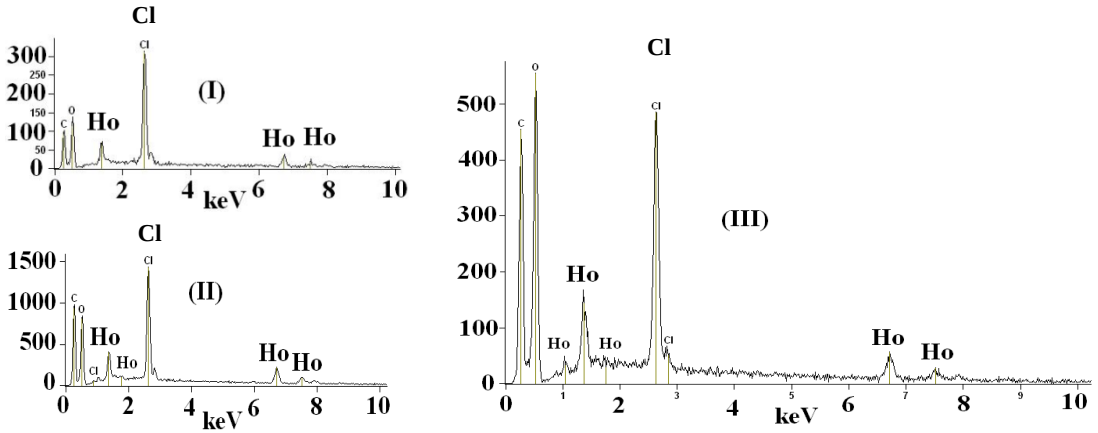

Figure 4: EDS of holmium loaded: (I) sample (B), a chitosan microsphere; (II) sample (D), a chitosan PVA blend; (III) sample (F), a chitosan-PVA cross-linked HPN.

3.4. Analysis by Confocal laser scanning microscopy (CLSM)

Scanning confocal microscopy, compared to most common techniques determining the morphology of microparticles such as scanning electron microscopy (SEM), has advantage of the confocal microscopy overcome limitations to acquire data which allows elucidation of mostly internal and external structures in the microparticles [26]. This technique offers a wide range of possibilities for elucidating morphological and three-dimensional views of the analyzed system, suitable to study polyelectrolyte chelating systems like chitosan interacting with Ho^{+3} ion. The green color of microspheres shown in Figures 5(I), (II), (III) corresponds to the fluorescence band emission of Ho^{3+} if is excited in the range of 450-490 nm, related to the decay of its "f" excited electrons. Once chitosan has yellow color, its absorption band reaches wavelengths of the sharp absorption bands associated to holmium ion excitations, so even the chitosan excited electrons can use unoccupied holmium electronic levels as ways to decay: this "antenna effect" may increase the intensity of the microparticles fluorescence [27,28], consistent to the experimental difficult to adjust the focus to take these images.

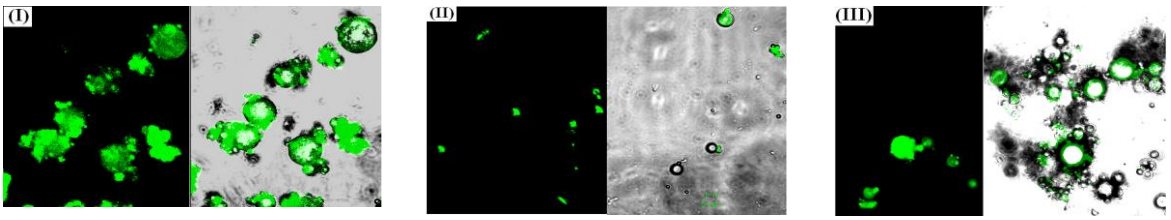

Figure 5: CLSM of $HoCl_3$ loaded microspheres of: (I) sample (B), a chitosan system; (II) sample (D) a chitosan-PVA blend; (III) sample (F), a chitosan-PVA cross-linked HPN.

3.5. Analysis by FTIR

IR spectroscopy was used to evaluate chemical groups of chitosan and PVA, and the samples (A-F). Related to free chitosan, its FTIR spectra follows in figure 6(I). Their peaks at 1550-1600 cm^{-1}, near of 1400 cm^{-1}, typically are assigned as carboxylate anion stretching modes: this indicates that chitosan acetate could be formed [26]; 3200-3600 cm^{-1} region corresponds normally to OH and NH_2 stretching modes [29]. According to literature, region around 3200-3570 cm^{-1} for chitosan [29], and 3200-3550 cm^{-1} for the PVA [12] (FTIR spectra in figure 6 (I)), have normal modes associated to the intermolecular and intramolecular interactions like hydrogen bonds between hydroxyl groups, or hydroxyl-amine kind. Finally, there are bands related to an eventual stretching mode of the hydroxyl groups related to absorbed water molecules in this region.

Chitosan cross-link with glutaraldehyde occurs from the nucleophilic amino group (NH_2) that reacts with the aldehyde carbon, displacing oxygen of it to loss water molecules and forms a C=N bond (~1648 cm^{-1}) of the Schiff base product [29,30]. If the environment pH of the reaction is neutral or alkaline it facilitates the existence of groups NH_2 (~1558 cm^{-1}) in the chitosan (pKa = 6.3), essential to obtain a Schiff base. In the acidic media, however, the NH_3^+ (~1548 cm^{-1}) is more likely to be formed: as it significantly reduces nitrogen nucleophilicity, it decreases the activity of Schiff base reaction. Literature suggests that glutaraldehyde cross-link preferably occurs via Schiff base formed at carbon 2 of the glycosidic ring, over the covalent bond with the hydroxyl groups on carbons 3 and 6. Usually 1730 cm^{-1} is attributed to a carbonyl stretching mode (C=O) of amides, and 1250 cm^{-1} which can be attributed to the -NH_3^+CO and OH bending due to a mixture of the polymers [29,31,32]. The 1648cm^{-1} band is attributed to the imine bond (C=N), and 1558 cm^{-1} is associated with the connection amine (NH_2); 1720 cm^{-1} is related to the free aldehyde groups (-COH) [33] - due the amount of glutaraldehyde added related to chitosan one, it is difficult to see the cross-link agent bands.

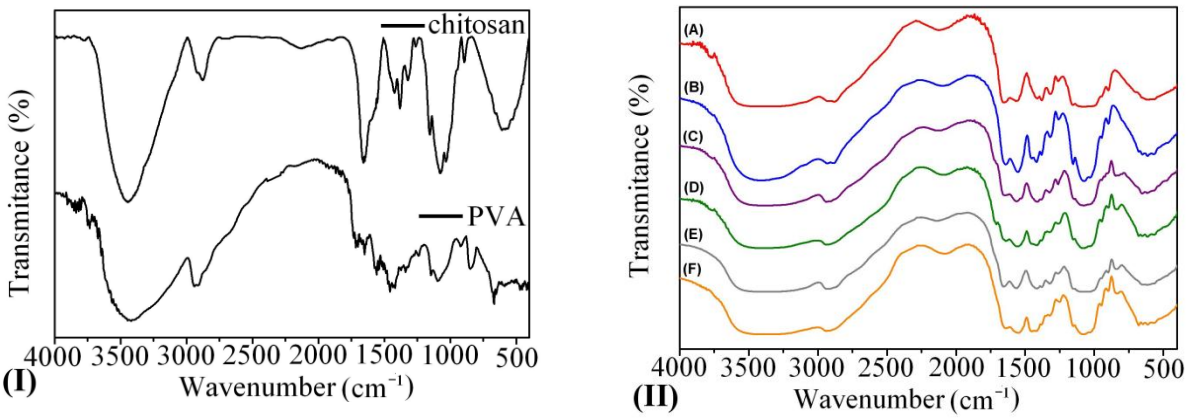

Figure 6: (I) Chitosan and PVA FTIR spectrum; (II) Comparative FTIR spectrum of the samples (A), (B), (C), (D), (E), (F). Each sample composition is described in table 1.

In spectrum (B), figure 6(II), the regions assigned to amine normal modes around 1560-1640cm^{-1} and 3200-3600 cm^{-1}, reveals absorption relatively smaller than (D) and (F) ones. Chitosan chains with higher degree of deacetylation as more flexible may facilitate hydrogen bond formation [34], so maybe there is more interaction between amine groups of chitosan and holmium in sample (B) than other samples because of absence of foreign polymer or

cross-link agent to react with NH_2 groups. Comparing spectrum (C) and (E), figure 6(II), around 1900-1500 cm^{-1}, range attributed to amide function, there is an increase in spectrum (E), figure 6(II): this may indicate that chitosan was reticulated by glutaraldehyde. The metal ions seem to interact with amorphous regions where the amine groups are located, as supported by the DRX patterns and confirmed by FTIR spectrometry.

3.6. Analysis by X-Ray Diffraction (XRD)

The use of X-ray diffraction allows differentiating chitin of chitosan and its deacetylated derivatives, crystallinity and provides information about the particles already used to analyze their size (item 3.2). In figure 7 (I) and (II) it's possible to see that all holmium loaded samples are more amorphous than the unloaded ones.

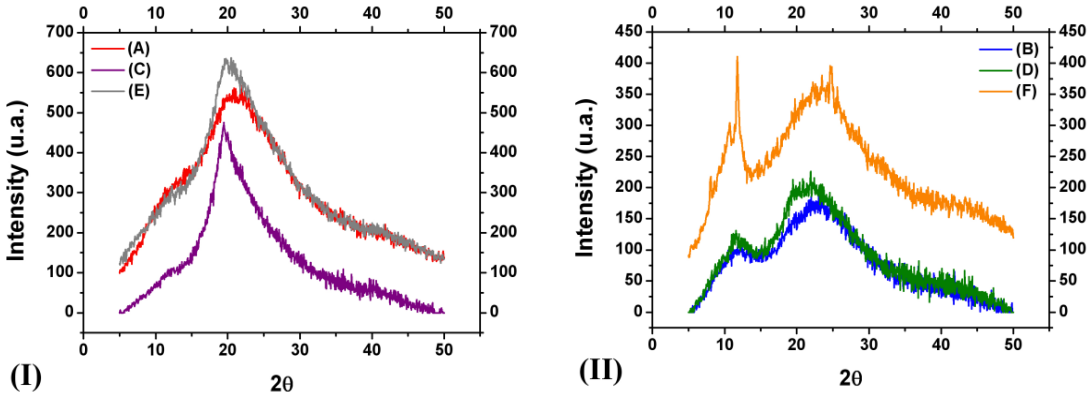

Figure 7: XRD diffractograms of (I) $HoCl_3$ unload microspheres: samples (A), (C) and (E); (II) $HoCl_3$ load microspheres: samples (B), (D) and (F).

As chitosan is deacetylated as lower existence of crystalline domains, and more amorphous is the polymer structure. This polymer and its derived networks usually exhibit structures semi-crystalline due to the free-energy balance caused by the formation of hydrogen bonding [29]. Chitosan chains with higher degree of deacetylation are more flexible, facilitating hydrogen bond formation and gain of crystallinity. The reflection around 10^o-11^o indicates the presence of a polymorphic crystal *form I* (orthorhombic crystal structure, its lattice parameters: a = 7.76 Å, b = 10.91 Å, c= 10.30 (along fiber axis) [33]); and the strongest reflection at $2\theta = 20^o$ corresponds to polymorphic crystal *form II* (crystal structure also orthorhombic and its lattice parameters a = 4.4 Å, b= 10.0 Å, c= 10.3 (along fiber axis) [33]) [34]. It is underlined that chitosan always contains bound water (5%) even if it has been extensively dried [35], hence the incorporation of bound water molecules into crystal lattice (hydrated crystals) generally gives rise to a more dominating polymorph which can be normally detected by a crystalline and broad peak in the corresponding X-ray pattern. The small crystalline peak around 10^o is attributed to the hydrated crystalline structure of chitosan, and the other near 20^o is reported as indication of the relatively regular crystal lattice of this polymer [36]. A tendency in all the prepared chitosan microspheres was that all the holmium load ones - samples (B), (D) and (F) - have diffractograms typical of a amorphous material, and peak intensity very low compared to the holmium unload ones - samples (A), (C) and (E). The crystalline index (I_{CR}) calculated to these last ones is, respectively, 36,16 %, 7,58 % and 50,07 %.

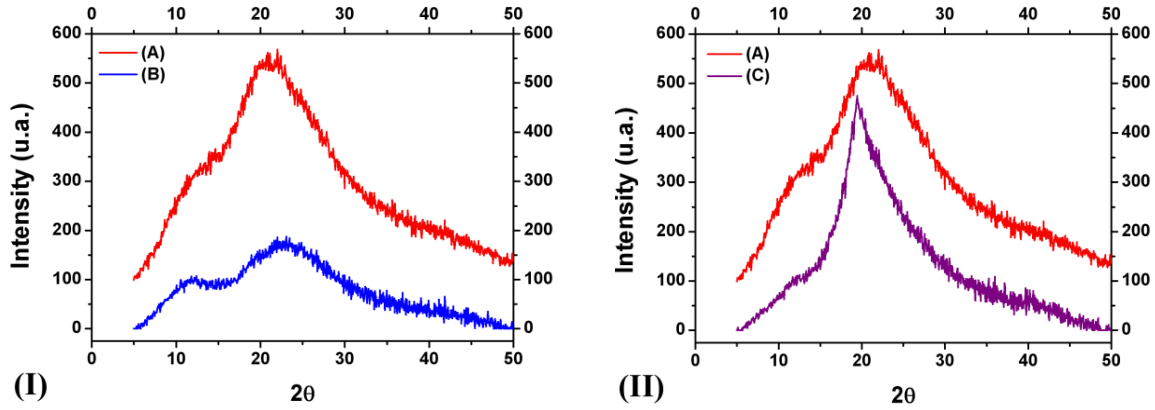

Figure 8. Comparison of XRD diffractograms: (I) sample (A), chitosan microspheres, and sample (B) $HoCl_3$ loaded chitosan microspheres; and (II) sample (A), chitosan microspheres, and sample (C) chitosan-PVA blend microspheres.

A three-dimensional conformation was suggested by Ogawa et al: polymorphic chitosan can easily change its conformation helix extended for another two laps for the formation of salts with acids or thermal treatment above 200°C [36]. In the figure 8(I), diffractogram of sample (B), that contains chitosan and holmium salt, its crystallinity decreased if compared to sample (A) one because this polymer is chelant: once complexed with Ho^{3+} these ions are interacting strongly with the polymer amino groups, and that results in a more amorphous system. In the figure 8(I), the peak around $2\theta = 10°$ in XDR of sample (B), attributed to the interaction of water [35] with the amino groups of chitosan, disappeared in the XDR of sample (C), figure 8(II); the change in this peak shows that its reflection has shifted to the left, forming a single peak, probably due the insertion of PVA chains in chitosan. It was suggested planar spacing structure to PVA, and the chain is also atactic trans conformation that have a strong maximum at $2\theta = 19.4°$ and a shoulder at $2\theta = 20°$, described as typical of the crystalline atactic PVA. [37]. The crystal structure is composed of double layers of molecules connected by hydrogen bonds, while weak Van der Waals forces act between the layers. Part of the chain structures in PVA leads to small ordered regions (crystallites) dispersed in an amorphous polymer matrix [37]. If the crystallites are homogeneously dispersed, because chitosan and PVA are very compatible polymers, then it can explain a single less intense and broad peak in sample (C) compared to (A). Due to direct interaction of hydroxyl groups of PVA with amino groups that were previously interacting with water, this new interaction may have modified the organization of the molecular structure of chitosan, leading to a possible decrease of the interplanar distance: this implies in an increased crystallinity, promoting a lower diffusion capacity to amorphous polymers.

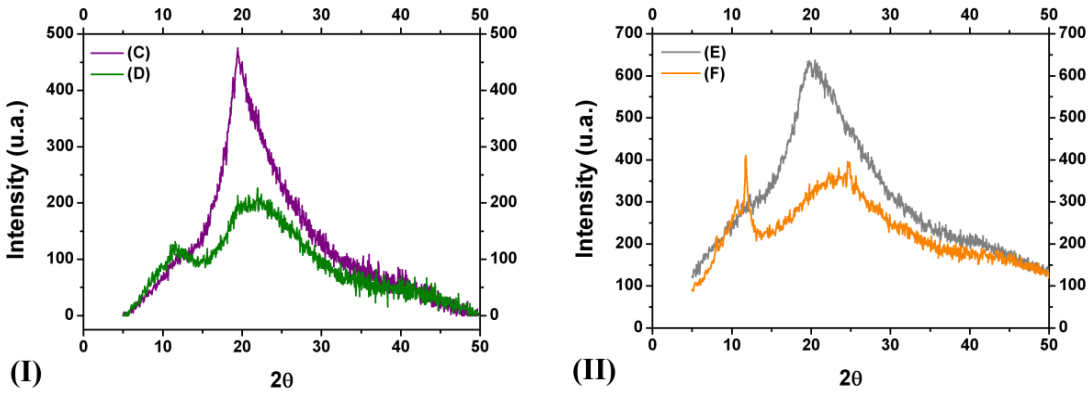

Figure 9. Comparison of XRD diffractograms: (I) sample (C), chitosan-PVA blend microspheres; and sample (D), $HoCl_3$ loaded chitosan-PVA blend microspheres; (II) sample chitosan-PVA blend microspheres; and sample (E) chitosan-PVA cross-linked microspheres.

In the figure 9(I), analyzing the diffractogram of sample (D) it is possible to see clearly that Ho^{3+} ions interacting with the amino groups of chitosan decrease very much its crystallinity compared to sample (C), probably because these ions are increasing the interplanar distance between PVA chains and chitosan chains, and also promoting higher diffusion capacity to amorphous polymers, allowing that amino groups interacts more directly with water. In the figure 9(II), it is possible to see that after chitosan and PVA are reticulated the peak around $2\theta = 19{,}7^{o}$ in the sample (E) was slightly shifted to right compared to the sample (C) one, and its intensity also increased. It is attributed probably because once glutaraldehyde cross-linked the polymers the interplanar distance between chains increased, and additionally the cross-linking and inter-cross-linking of interpenetrated polymer chains decreased dramatically the system randomness. This can explain the observe gain in the microspheres crystallinity.

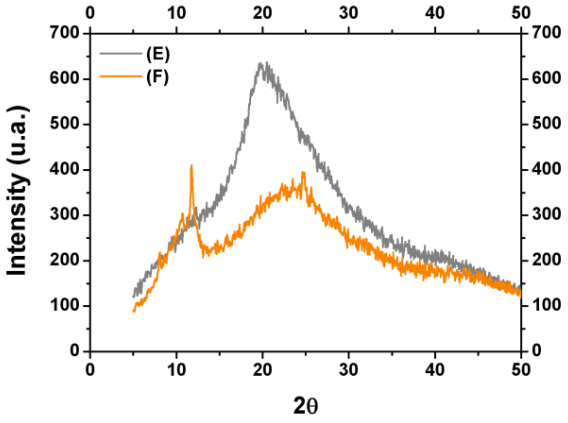

Figure 10. Comparison of XRD diffractograms: (I) sample (E), chitosan-PVA cross-linked microspheres; and (II) sample (F) $HoCl_3$ load chitosan-PVA cross-linked microspheres.

In the figure 10, is possible to verify that $HoCl_3$ presence in sample (F) seems to increase interplanar distance between the chitosan and PVA chains, hence decreasing the microsphere crystallinity. The lanthanide ions seem to interact particularly with amino group in disordered portions of the chitosan. This is evidenced by changes in the $9^{o} < 2\theta < 13^{o}$ peak as a function of the chelated metal ion. According to Webster et al, chitosan-glutaraldehyde may be in a

form of two chitosan chains in the antiparallel fashion connected with two imino nitrogens of C-2 to the antiparallel chitosan chains. The aldehyde groups of glutaraldehyde are displaced by the nitrogens forming a Schiff's base. Therefore, surface area of chitosan-glutaraldehyde relative to chitosan is larger, but the cross-linking increased the competition of metal-binding nitrogen sites, which decreases the metal uptake ability in chitosan-glutaraldehyde [11] – and it is consistent to the gain of size in the microspheres.

3.4. Analysis by TGA

The chitosan microspheres degradation temperature is lower than pure polymer: chitosan start to degrade at 300°C, figure 11. Degradation temperatures of sample (B), a $HoCl_3$ loaded microsphere is 281°C, showed this event in higher temperatures than sample (A) one, 261ºC: that can be related to Ho^{+3} chelation enhancing the stability of the system. By the other side, the samples (C) and (D) didn't show any difference in their degradation temperature (247ºC), no matter if it is an $HoCl_3$ unloaded or loaded one, but PVA presence in these microsphere compositions decreased their degradation temperature. This reveals that, despite of the gain in solubility and easy of processing - other possible explanation of smaller microspheres than a cross-linked system - the blended system has stability smaller than a HPN one.

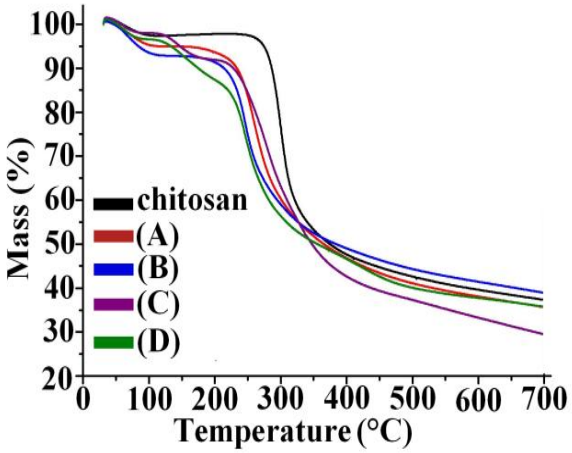

Figure 11: Chitosan Sigma Aldrich , samples (A), (B), (C), (D), (are described in table 1).

3. CONCLUSIONS

The preliminary results showed that chitosan microspheres loaded with holmium-165 were formed by Spray Dryer method, as can be seen in the SEM images. The EDS and CLSM studies confirmed the presence of holmium in the prepared microspheres, and a homogenous distribution in them. TGA analysis showed that microspheres produced by Spray Dryer has degradation temperatures lower than pure chitosan, and in a chitosan-PVA blend ones this event occurs in smaller temperatures; more studies with microspheres produced from HPNs of chitosan-PVA cross-linked with glutaraldehyde are necessary. XRD analysis indicates that samples (E) and (F) are more suitable for brachytherapy to treat prostate cancer, rheumatoid arthritis and many other applications due their better crystallinity related to the other systems prepared.

ACKNOWLEDGMENTS

We would like to thank Eleosmar Gasparin CQMA/IPEN-CNEN for thermal analysis, Celso Vieira CCTM/IPEN-CNEN for SEM images, Adriana Napoleão Geraldes CQMA/IPEN-CNEN for DRX analysis, José R. Martinelli CCTM/IPEN-CNEN for particle size analysis**.**
Financial Support: DIRF/IPEN/CNEN; MCT/CNPq 550598/2010-3; 310227/2010-0; 381405/2011-7; 111795/2011-7.

REFERENCES

1. C. Qin, Y. Du, L. Xiao, Z. Li, and X. Gao, "Enzymic preparationof water-soluble chitosan and their antitumor activity", *International Journal of Biological Macromolecules*, **31**, pp. 111-117 (2002).
2. C. Kwak, S. K. Hong, S. K. Seong, J. M. Ryu, M. S. Park, and S. E. Lee, "Effective local control of prostate cancer by intratumoral injection of ^{166}Ho-chitosan complex (DW-166HC) in rats", *European Journal of Nuclear Medicine and Molecular Imaging*, **32**, pp.1400-1405 (2005).
3. J. Song, C. H. Suh, Y. B. Park, S. H. Lee, N. C. Yoo, J. D. Lee, S. K. Lee, and K. H. Kim, "A phase I/IIa study on intra-articular injection of holmium-166-chitosan complex for the treatment of knee synovitis of rheumatoid arthritis", *European Journal of Nuclear Medicine*, **28**, pp.489-497 (2001).
4. Lifeng Qi, and Zirong Xu, "In vivo antitumor activity of chitosan nanoparticles", *Bioorganic & Medicinal Chemistry Letters*, 16, pp.4243-4245, 2006.
5. M. Dash, F. Chiellini, R.M. Ottenbrite, and E. Chiellini, "Chitosan - A versatile semi-synthetic polymer in biomedical applications", *Progress in Polymer Science*, **36**, pp.981-1014 (2011).
6. Renata F. Costa, Mariangela B. M. Azevedo, Nanci Nascimento, Frank F. Sene, José R. Martinelli, João A. Osso International Nuclear Atlantic Conference - INAC 2009; Associação Brasileira de Energia Nuclear - ABEN ISBN**:** 978-85-99141-03-8.
7. B. KRAJEWSKA, "Synthesis, characterization and controlled drug release of thermosensitive IPN–PNIPAAm hydrogels", *Biomaterials*, **25**, pp. 3793-3805 (2004).
8. I. R. Rodrigues, "Síntese e caracterização de redes poliméricas à base de quitosana com PVP e PVA para aplicação na liberação controlada de fármacos", Dissertação de Mestrado; Universidade Federal do Rio Grande do Sul, Porto Alegre, 2006.
9. L. M. Guerrini, M. C. Branciforti, R. E. S. Bretãs, and M. P. de Oliveira, "Eletrofiação do poli(álcool vinílico) via solução aquosa", *Polímeros: Ciência e Tecnologia*, **16**, pp.286-293 (2006).
10. L. E. Udrea, D. Hritcu, M. I. Popa, and O. Rotariu, "Preparation and characterization of polyvinyl alcohol-chitosan biocompatible magnetic microparticles", *Journal of Magnetism and Magnetic Materials*, **323**, pp.7–13 (2011).
11. A. Webster, Merrill D. Halling and David M. Grant, "Metal complexation of chitosan and its glutaraldehyde cross-linked derivative", *Carbohydrate Research*, **342**, pp.1189-1201 (2007).
12. H. S. Mansur, C. M. Sadahira, A. N. Souza, and A. A. P. Mansur, "FTIR spectroscopy characterization of poly (vinyl alcohol) hydrogel with different hydrolysis degree and chemically crosslinked with glutaraldehyde", *Materials Science and Engineering C*, **28**, pp.539–548 (2008).
13. H.L. Frisch, D. Klempner, K.C. Frisch, "A topologically interpenetrating network", *Journal of Polymer Science Part B: Polymer Letters*. **7**, 775-779 (1696).

14. L.H. Sperling, D.W. Friedman, "Synthesis and Mechanical Behavior of Interpenetrating Polymer Networks: Poly(ethyl Acrylate) and Polystyrene, *Journal of Polymer Science A-2: Polymer Physics*, **7**, pp.425-427 (1969).
15. P.K. Pandyopadhyay, M.T. Shaw, "Viscoelastic and engineering properties of poly(vinyl chloride) plasticized with polycaprolactone-based polyurethanes", *Journal of Applied Polymer Science*, **27**, pp.4323-4335 (1982).
16. A.A. Donatelli, D.A. Thomas, and L.H. Sperling, "Poly (butadiene-co-styrene)/polystyrene IPNs, semi-IPNs and graft copolymers: Staining behavior and morphology", *Polymer Science and Technology*, **1**, pp.4375-4393 (1974).
17. J. Berger, M. Reist, J.M. Mayer, O. Felt, N.A. Peppas, and R. Gurny, "Structure and interactions in covalently and ionically crosslinked chitosan hydrogels for biomedical applications", *European Journal of Pharmaceutics and Biopharmaceutics*, **57**, pp.19-34 (2004).
18. X. Li , N. Anton, C. Arpagaus, F. Belleteix , T.F. Vandamme, "Nanoparticles by spray drying using innovative new technology: The Büchi Nano Spray Dryer B-90", *Journal of Controlled Release,* **147,** pp.304–310 (2010).
19. A. Grenha, B. Seijo, C. Serra, and C. Remuán-López., "Chitosan nanoparticle-loaded mannitol microspheres: structure and surface characterization", *Biomacromolecules*, **8**, pp.2072–2079 (2007).
20. H.Y. Huang, Y.T. Shieh, C.M. Shih, and Y.K. Twu., "Magnetic chitosan/iron (II, III) oxide nanoparticles prepared by spray-drying", *Carbohydrate Polymer*, **81**, pp.906–910 (2010).
21. L. Vitali, M. C. M. Laranjeira, V. T. Fávere, "MICROENCAPSULAÇÃO DO AGENTE QUELANTE SULFOXINA EM MICROESFERAS DE QUITOSANA PREPARADAS POR SPRAY DRYING COMO NOVO ADSORVENTE PARA ÍONS METÁLICOS", *Quimica Nova*, **Vol. 31**, No. 6, p. 1400-1404 (2008).
22. Li, J. -F. Revol, and R. H. Marchessault, "Effect of Degree of Deacetylation of Chitin on the Properties of Chitin Crystallites", *Journal of Applied Polymer Science,* **65**, pp.373-380 (1997).
23. R. Signini, and F. S. P. Campana, "Características e propriedades de quitosanas purificadas nas formas neutra acetato e cloridrato", *Polímeros: Ciência e Tecnologia*, **11**, pp. 58-64 (2001).
24. A. Lamprecht, U. Schäfer, and C.M. Lehr, "Structural Analysis of Microparticles by Confocal Laser Scanning Microscopy", *American Association of Pharmaceutical Scientists PharmSciTech*, **1**(3), article 17 (2000).
25. D. G. Karroker, "Coordination of Trivalent Lanthanide Ions", *Journal of Chemical Education,* **Vol. 47, N.** 6**,** (1970).
26. S. Harikarnpakdee, V. Lipipun, N. Sutanthavibul, and G.C. Ritthidej, "Spray-dried Mucoadhesive Microspheres: Preparation and Transport Through Nasal Cell Monolayer", *American Association of Pharmaceutical Scientists PharmSciTech*, (1), article 12, (2006).
27. S. Dang, J.Yu, X. Wang., L. Sun, R. Deng, J. Feng, W. Fan, H. Zhang, "NIR-luminescencefromternarylanthanide[HoIII, PrIII and TmIII] complexes with 1-(2-naphthyl)-4,4,4-trifluoro-1,3-butanedionate ", *Journal of Luminescence*, **vol.131**, p. 1857–1863 (2011).
28. J.G. Bunzli, C. Piguet, "Taking advantage of luminescent lanthanide ions", *Chemical Society Reviews*, **vol.34**, p. 1048-1077 (2005).
29. E. S. Costa-Junior, E. F. Barbosa-Stancioli, A. A. P. Mansur, W. L. Vasconcelos, and H. S. Mansur, "Preparation and characterization of chitosan/poly(vinyl alcohol) chemically crosslinked blends for biomedical applications", *Carbohydrate Polymers*, **76**, pp.472–481 (2009).

30. A. P. Rokhade, N. B. Shelke, S. A. Patil, and T. M. Aminabhavi, “Novel interpenetrating polymer network microspheres of chitosan and methylcellulose for controlled release of theophylline”, *Carbohydrate Polymers*, **69**, pp.678-687 (2007).
31. T. Wang, M. Turhan, and S. Gunasekaran, “Selected properties of pH-sensitive, biodegradable chitosan-poly(vinyl alcohol) hydrogel”, *Polymer International*, **53**, pp.911-918 (2004).
32. P.S. Rao, B. Sumitha, S. Sridhar, A. Krishnaiah, “Preparation and performance of poly(vinyl alcohol)/polyethyleneimine blend membranes for the dehydration of 1,4-dioxane by pervaporation: Comparison with glutaraldehyde cross-linked membranes”, *Separation and Purification Technology*, **48**, pp.244-254 (2006).
33. K. Girdhari, “Developmente and characterization of novel organic coating based on biopolymer chitosan”, Dissertation to obtain Degree Doctor of Philosophy in the Graduate School of The Ohio State University, (2006).
34. C. Zhang, Y. Ding, Q. Ping, and L. L. Yu, “Novel chitosan-derived nanomaterials and their micelle-forming properties”, *Journal of Agricultural and Food Chemistry*, **54**, pp.8409-8416 (2006).
35. B. W. S. Souza, M.A. Cerqueira, J.T. Martins, A. Casariego, J.A. Teixeira, and A.A. Vicente, “Influence of electric fields on the structure of chitosan edible coatings”, *Food Hydrocolloids*, **24**, pp.330–335 (2010).
36. K. Ogawa, T. Yui and K. Okuyama, “Three D structures of chitosan”, *International Journal of Biological Macromolecules*, **34**, pp.1-8 (2004).
37. R. Ricciardi, F. Auriemma, C. De Rosa, F. Lauprêtre, “X-ray Diffraction Analysis of Poly(vinyl alcohol) Hydrogels, Obtained by Freezing and Thawing Techniques”, *Macromolecules*, **vol.** ***37****, p.*1921-1927 (2004).
38. G. A. S Goulart, “Obtenção e caracterização de micropartículas de quitosana contendo papaína”; Tese de Doutorado, Universidade Estadual de Campinas, São Paulo, Campinas, 2006.